

## Article

# Comparative Analysis of Primary and Secondary Emission Mitigation Measures for Small-Scale Wood Chip Combustion

Christian Gollmer <sup>\*</sup>, Theresa Siegmund , Vanessa Weigel and Martin Kaltschmitt 

Institute of Environmental Technology and Energy Economics, Hamburg University of Technology (TUHH), Eissendorfer Strasse 40, 21073 Hamburg, Germany; theresa.siegmund@tuhh.de (T.S.); kaltschmitt@tuhh.de (M.K.)  
\* Correspondence: christian.gollmer@tuhh.de; Tel.: +49-40-42878-3319; Fax: +49-40-42878-2315

**Abstract:** The objective of this study is to systematically investigate not only the influence of different additive types—beyond the much-considered case of aluminum-silicate-based additives—but also to carry out an additional comparison between primary and secondary emission mitigation measures during small-scale wood-chip combustion. Hence, combustion trials are realized within a 33-kW combustion plant. Pine wood chips additivated with 1.0 wt%<sub>a.r.</sub> of four additives have shown promising emission reduction effects in the past; namely kaolin (i.e., aluminum-silicate-based), anorthite (i.e., aluminum-silicate- and calcium-based), aluminum hydroxide (i.e., aluminum-based), and titanium dioxide (i.e., titanium-based). In addition to the primary mitigation measure (i.e., (fuel) additivation), an electrostatic precipitator (ESP) as a common secondary mitigation measure for total particulate matter (TPM) reduction is used for comparison. In addition to standard analyses (e.g., gravimetric determination of TPM emissions), an extended methodology (e.g., characterization of the elemental composition and ultrafine particle fraction of TPM emissions) is applied. The results show that the additivation of wood chips with kaolin and anorthite can lead to an operation of the combustion plant in compliance with the German legal TPM limit values by undercutting the absolute emission level achievable by the ESP. Additionally, kaolin and anorthite achieve significant reductions in carbon monoxide (CO) emissions, while kaolin simultaneously, and similarly to ESP, also leads to a shift in the particle size number distribution of PM emissions towards coarser particles. All additives show a significant reduction of potassium (K) emissions by the formation of high-temperature stable K compounds in the resulting ashes.



**Citation:** Gollmer, C.; Siegmund, T.; Weigel, V.; Kaltschmitt, M. Comparative Analysis of Primary and Secondary Emission Mitigation Measures for Small-Scale Wood Chip Combustion. *Energies* **2024**, *17*, 4403. <https://doi.org/10.3390/en17174403>

Academic Editor: Dariusz Kardas

Received: 15 August 2024

Revised: 28 August 2024

Accepted: 1 September 2024

Published: 3 September 2024



**Copyright:** © 2024 by the authors. Licensee MDPI, Basel, Switzerland. This article is an open access article distributed under the terms and conditions of the Creative Commons Attribution (CC BY) license (<https://creativecommons.org/licenses/by/4.0/>).

**Keywords:** wood chips; combustion; emissions; fuel additivation; electrostatic precipitator; total particulate matter; ultrafine particulate matter; carbon monoxide

## 1. Introduction

The energetic utilization of wood fuels (e.g., wood pellets, wood logs, and/or wood chips) for the provision of (domestic) heat in small-scale combustion plants is associated with the formation of air pollutants (e.g., particulate matter (PM) and carbon monoxide (CO)) [1–5]. Due to the potentially harmful impact on human health and the environment, these PM and CO emissions are subject to legal limits [1,6,7]. Larger combustion plants (e.g., combined heat and power plants fired with biomass) address the issue of PM emissions with (expensive) secondary mitigation measures (e.g., a baghouse filter or electrostatic precipitator (ESP)). Such measures are usually not economically feasible for small-scale combustion plants (i.e., up to 1000 kW) [1,6,8–10]. For this reason, primary or fuel-side PM mitigation measures have been intensively investigated for smaller appliances so far; for example, optimization of the combustion chamber design, utilization of fuel/combustion air staging or flue gas recirculation, and/or modification of the solid biofuels itself [1,10–12].

A frequently considered primary mitigation measure, especially for the reduction of (inorganic) PM emissions, is the addition of so-called additives to solid wood fuels (i.e., (fuel) additivation) [13–15]. Such additives are usually minerals or chemical compounds

capable of changing the chemistry of the ash, reducing the level of harmful emissions (e.g., PM, CO), and/or increasing the melting temperature of the ash [14,15]. In the case of an almost complete combustion of solid biofuels in modern (small-scale) combustion units, PM emissions originate mainly from the inorganic components of the wood fuel [16–19]. Among these inorganic wood components, the ash- and PM-forming alkali element potassium (K) is of particular importance [18–22]. Depending on the chemical composition of the wood fuel and the combustion parameters (e.g., temperature, time, turbulence), K is primarily volatilized as gaseous species (e.g., potassium hydroxide (KOH), potassium chloride (KCl), potassium sulfate ( $K_2SO_4$ ), and/or potassium carbonate ( $K_2CO_3$ )) to the flue gas [23–26]. Due to cooling effects in the stack or in the atmosphere, these K compounds are converted back into a solid phase and ultimately form the main part of non-organic PM emissions released into the environment [23–26].

Based on the main reactive element influencing the formation of the inorganic or K-related PM emissions, additives can be classified as (1) aluminum-silicate-based, (2) calcium-based, (3) phosphorus-based, and (4) other type additives (e.g., titanium-based) [13–15]. The effect of aluminum-silicate-based additives is essentially based on the (irreversible) chemical reaction of the additives with the highly volatile K compounds (e.g., KOH, KCl, and  $K_2SO_4$ ) [15,24,25]. The declared aim is to convert the K compounds released typically in a gaseous form during the combustion of the solid biofuel into temperature-stable compounds (i.e., kalsilite ( $KAlSiO_4$ ), leucite ( $KAlSi_2O_6$ ), and/or orthoclase/microcline ( $KAlSi_3O_8$ )) via a series of (heterogeneous) gas-solid or liquid-solid reactions [13–15]. A common example of an aluminum-silicate-based additive is kaolin or the pure, mineral form of kaolin known as kaolinite ( $Al_2Si_2O_5(OH)_4$ ) [13–15,27]. Solely aluminum-based additives (e.g., bauxite) have also been investigated for their reaction behavior with respect to the gaseous K compounds (e.g., KOH, KCl,  $K_2SO_4$ ) [28,29]. While the (ash) incorporation of K by aluminum-silicate-based additives (e.g., kaolin) is based on an (irreversible) chemical reaction mechanism, the underlying process of the aluminum-based additive bauxite is also considered, at least in part, to be a (reversible) physical mechanism (i.e., physical adsorption) [28,29].

Calcium-based additives include calcium carbonate ( $CaCO_3$ ), calcium oxide (CaO), calcium hydroxide ( $Ca(OH)_2$ ), and/or those substances that in principle contain the previously mentioned calcium compounds (e.g., dolomite ( $CaMg(CO_3)_2$ )) [14,15,30,31]. An important property of calcium-based additives is the increase of the ash melting point of additivated solid biomasses [14,30,32]. However, for phosphate-containing biomasses, especially in the presence of K-rich phosphates with low melting points (e.g.,  $KPO_3$ ,  $KH_2PO_4$ ), it has been demonstrated that the use of calcium carbonate, calcium oxide, or calcium hydroxide, among others, leads to an improvement of the ash-melting behavior by forming different K calcium phosphates (e.g.,  $KCaPO_4$ ,  $KCa_{10}(PO_4)_7$ ) with high melting temperatures in the ash [27,33–36]. Thus, calcium-based additives tend to be more effective in combination with phosphorus- and K-containing biomasses [14,15,37].

Accordingly, phosphorus-based additives are discussed especially for solid biofuels with a high content of K and silicon and a moderate content of alkaline earth elements (i.e., calcium and magnesium) [13–15].

In addition to these additives, further elements, compounds, or minerals (e.g., titanium-based, sulfur-based, and magnesium-based) are considered in the literature to influence the ash-melting behavior and/or the release of highly volatile, PM-forming K compounds (i.e., KOH, KCl,  $K_2SO_4$ ) [32,38–46]. Titanium-based additives that can be used in the combustion of biomass include titanium dioxide ( $TiO_2$ ) or the mineral ilmenite ( $FeTiO_3$ ) [39,41]. It has been shown that the ash- and PM-forming K or K compounds can react with ilmenite to form K titanium oxides or K titanates (e.g.,  $KTi_8O_{16}$ ) and, thus, titanium-based additives are considered to have the fundamental ability to incorporate K in the ash [39].

The use of additives has already been extensively investigated for the combustion of (wood) pellets in small-scale combustion plants [14,20,30,33,47–49]. Here, the additives are usually added during pellet production (e.g., within the pelletizing process) by mixing

after pellet production (e.g., within the fuel feeding system) or by direct injection into the combustion plant (e.g., via the combustion air or separate spraying systems) [15].

In contrast to (wood) pellets, the data for harmful emission mitigation (e.g., PM, CO) by additivation during small-scale wood-chip combustion are currently still very limited [49,50]. This is despite the fact that, for example, smaller wood-chip appliances with an automatic fuel supply that were built after 1 January 2015, must comply with the legal limits of 20 mg/Nm<sup>3</sup> for PM emissions and of 400 mg/Nm<sup>3</sup> for CO emissions in Germany according to the 1. BImSchV [51]. Similar legal constraints are also valid in other European countries.

Thus, the objective of this paper is to systematically analyze the transferability of fuel additivation as a primary mitigation measure for K-based PM emissions during wood-chip combustion. Therefore, combustion trials are performed in a combustion plant (33 kW) with automatic wood-chip feeding. These wood chips are additivated with 1.0 wt%<sub>a.r.</sub> (a.r.: wood chips as received) of different additives shown promising effects in terms of potential emission reduction [52], namely kaolin (i.e., aluminum-silicate-based), anorthite (i.e., aluminum-silicate- and calcium-based), aluminum hydroxide (i.e., aluminum-based) and titanium dioxide (i.e., titanium-based). To evaluate the additivation within the combustion trials, the total particulate matter (TPM) emissions are considered. Furthermore, the K emissions and the (ultrafine) particulate matter (PM<sub>(0.1)</sub>) emissions are also investigated as sub-fractions of the TPM emissions. As a gaseous component of the flue gas, the CO emissions are analyzed as well. Finally, the chemical composition of the ashes from the combustion of the (additivated) wood chips is further characterized. In addition to the mitigation measure of (fuel) additivation, an ESP is used for comparison purposes as a common secondary mitigation measure for PM reduction.

Consequently, the present study investigates not only the influence of different additive types—beyond the often-considered case of aluminum-silicate-based additives—but also draws an additional comparison between primary and secondary emission mitigation measures. Additionally, the present study goes beyond standard analyses of wood combustion emissions (e.g., gravimetric determination of TPM emissions) by applying an extended methodology (e.g., characterization of the chemical composition and ultrafine particle fraction of the TPM emissions). It thus provides a deeper understanding of the potential air quality impacts of a conventional small-scale combustion plant as well as promising mitigation approaches with respect to more stringent air pollution limits for woody fuel combustion in the future.

## 2. Material and Methods

The experimental design involved the (fuel) additivation of pine wood chips with 1.0 wt%<sub>a.r.</sub> of the four additives kaolin, anorthite, aluminum hydroxide, and titanium dioxide. The additive content was derived from stoichiometric calculations and preliminary investigations [49,52,53]. The additivation of the fuel was carried out according to an already established procedure by mixing an appropriate amount of the wood chips with 1.0 wt%<sub>a.r.</sub> of the respective additive for 10 min in a rotating concrete mixer [54]. In total, six samples were prepared (Table 1); one for each additive, a reference sample without any additive, and an additional non-additivated sample of pure wood chips for combustion trials with ESP. The (non-)additivated wood chips were subsequently burned in a 33-kW combustion plant and released emissions were measured. For all combustion trials (i.e., without and with an additive), the TPM emissions (incl. chemical composition), the K emissions, the PM<sub>(0.1)</sub> emissions, the CO emissions, and the resulting ashes (incl. chemical composition and crystalline phases) were analyzed. In the following, the experimental setup used and the analytical methodology applied are presented.

**Table 1.** Denotation of the wood-chip samples and combustion trials (a.r.: wood chips as received).

Sample Name	Biomass	Mitigation Measure
Without Additive	Pine wood chips	–
Kaolin	Pine wood chips	1 wt% <sub>a.r.</sub> Kaolin
Anorthite	Pine wood chips	1 wt% <sub>a.r.</sub> Anorthite
Aluminum hydroxide	Pine wood chips	1 wt% <sub>a.r.</sub> Aluminum hydroxide
Titanium dioxide	Pine wood chips	1 wt% <sub>a.r.</sub> Titanium dioxide
ESP	Pine wood chips	Electrostatic precipitator

### 2.1. Wood Chips

Barkless pine wood chips were used as solid biofuels for the analyses and investigations. The untreated wood chips were provided by a fuel supplier in the North of Germany (Lüneburg, Germany). The fuel properties and chemical composition of the pine wood chips are shown in Table 2 [55–57].

**Table 2.** Fuel properties and chemical composition of the pine wood chips (a.r.: wood chips as received, d.b. dry wood chip basis, \*: calculated by mass difference, n.d.: not determined).

Parameter	Unit	Wood Chips
Moisture content	wt% <sub>a.r.</sub>	8.1
Ash content	wt% <sub>d.b.</sub>	0.3
Carbon (C)	wt% <sub>d.b.</sub>	49.0
Hydrogen (H)	wt% <sub>d.b.</sub>	6.7
Oxygen (O) *	wt% <sub>d.b.</sub>	43.4
Nitrogen (N)	wt% <sub>d.b.</sub>	<0.1
Sulphur (S)	wt% <sub>d.b.</sub>	<0.2
Potassium (K)	mg/kg <sub>d.b.</sub>	290
Sodium (Na)	mg/kg <sub>d.b.</sub>	<5
Calcium (Ca)	mg/kg <sub>d.b.</sub>	709
Magnesium (Mg)	mg/kg <sub>d.b.</sub>	155
Silicon (Si)	mg/kg <sub>d.b.</sub>	n.d.
Manganese (Mn)	mg/kg <sub>d.b.</sub>	29
Phosphorus (P)	mg/kg <sub>d.b.</sub>	n.d.
Aluminum (Al)	mg/kg <sub>d.b.</sub>	18
Iron (Fe)	mg/kg <sub>d.b.</sub>	12
Copper (Cu)	mg/kg <sub>d.b.</sub>	7
Zinc (Zn)	mg/kg <sub>d.b.</sub>	6
Lead (Pb)	mg/kg <sub>d.b.</sub>	<1

According to the applicable fuel norm, the utilized wood chips had a typical chemical composition for untreated, coniferous solid biofuels (i.e., without significant amounts of bark and/or needles) [58–60]. Based on the determined fuel properties (i.e., water and ash content), a quality classification of A1 could be derived for the used wood chips [59].

### 2.2. Additives

The additives were selected based on thermodynamic equilibrium calculations using FactSage 7.1 [61] as well as our own laboratory-scale investigations [52]. Kaolin (i.e., main component kaolinite ( $\text{Al}_2\text{Si}_2\text{O}_5(\text{OH})_4$ )) was used as a widely established aluminum-silicate-based additive, while anorthite ( $\text{CaAl}_2\text{Si}_2\text{O}_8$ ) was used as a hybrid of the aluminum-silicate- and calcium-based additives. In preliminary studies, both additives showed a pronounced high-temperature stable ash incorporation or recovery rate of K in corresponding biomass-additive samples for a temperature of 1100 °C [52]. A comparable, potentially promising (inorganic) TPM mitigation effect was also demonstrated for the exclusively aluminum-based aluminum hydroxide [52]. High-temperature, stable K compounds (e.g.,  $\text{K}_2\text{TiO}_3$ ) were also detected for titanium dioxide in biomass-additive ashes (1100 °C); although, the associated recovery rate for K was significantly lower compared to the other additives (i.e.,

kaolin, anorthite, and aluminum hydroxide) [52]. The aluminum-silicate-based additive kaolin was provided by Gebrüder Dorfner GmbH & Co. Kaolin- und Kristallquarzsand-Werke KG (Hirschau, Germany) [62]. The additives anorthite and aluminum hydroxide were delivered by Andrea Wolbring GmbH & Co. KG (Anzing, Germany) [63,64], while the titanium dioxide was obtained from VWR International LLC (Darmstadt, Germany) [65]. The chemical compositions of the additives used are shown in Table 3 [62–65], while Figure 1 shows the corresponding cumulative particle size mass distributions.

**Table 3.** Chemical composition of the additives kaolin, anorthite, aluminum hydroxide, and titanium dioxide (a.r.: additives as received).

Parameter	Unit	Kaolin	Anorthite	Aluminum Hydroxide	Titanium Dioxide
SiO <sub>2</sub>	wt% <sub>a.r.</sub>	50.2	43.2	–	–
Al <sub>2</sub> O <sub>3</sub>	wt% <sub>a.r.</sub>	34.4	36.6	65.4	–
H <sub>2</sub> O	wt% <sub>a.r.</sub>	12.0	20.2	34.6	–
CaO	wt% <sub>a.r.</sub>	<0.1	–	–	–
TiO <sub>2</sub>	wt% <sub>a.r.</sub>	0.4	–	–	100.0
Fe <sub>2</sub> O <sub>3</sub>	wt% <sub>a.r.</sub>	0.5	–	–	–
K <sub>2</sub> O	wt% <sub>a.r.</sub>	2.1	–	–	–
Na <sub>2</sub> O	wt% <sub>a.r.</sub>	0.2	–	–	–
MgO	wt% <sub>a.r.</sub>	<0.1	–	–	–
P <sub>2</sub> O <sub>5</sub>	wt% <sub>a.r.</sub>	0.2	–	–	–

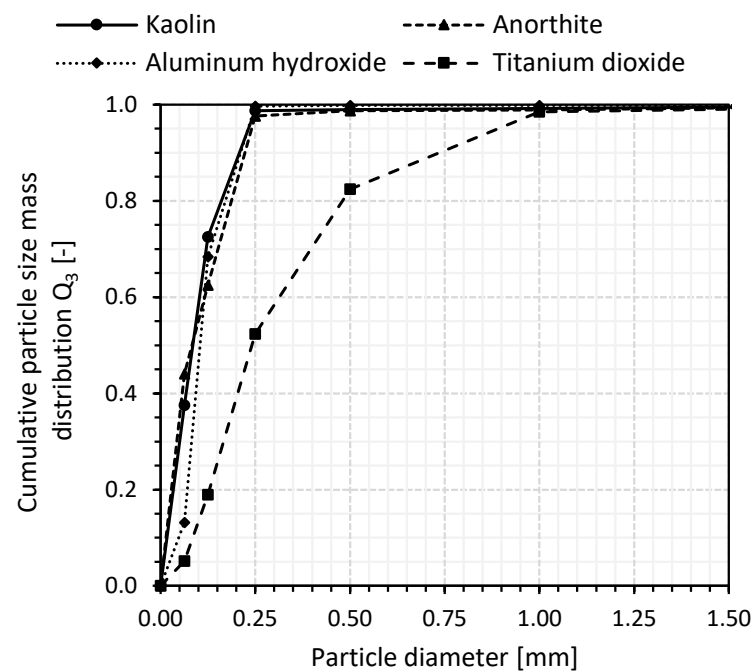


**Figure 1.** Cumulative particle size mass distribution of the additives kaolin, anorthite, aluminum hydroxide, and titanium dioxide.

### 2.3. Combustion Plant

For the combustion trials, a 33-kW combustion plant from the company Heizomat (Gunzenhausen, Germany) (i.e., RHK-AK boiler series) was utilized. The grateless RHK-AK 30 [66] boiler was designed with an automatic fuel supply (e.g., for pellets and wood chips) and glow-bar ignition. A patented ash removal system ensures automatic ash discharge during operation. The plant control and the visualization of the furnace parameters were carried out by means of the Heizococontrol ET200 system (Heizomat-

Gerätebau + Energiesysteme GmbH, Gunzenhausen, Germany). In addition, the combustion plant was equipped with an EF 185 ESP, which can be optionally switched on or off.

A measuring section according to DIN EN 15259 [67] (Figure 2) was connected to the combustion plant, which could be used to analyze the emissions (e.g., TPM,  $PM_{(0.1)}$ , CO) during the combustion of the solid biofuels (e.g., wood chips). Prior to each combustion trial, the combustion chamber, the automatic fuel feed system, and the fuel bunker were cleaned to remove any residues from previous test runs. For each combustion test, the empty fuel bunker of the combustion plant was loaded with approximately 60 kg of the wood chips to be tested (i.e., non-additivated for the reference measurement and the use of the ESP or additivated with 1.0 wt.%<sub>a.r.</sub> of each of the four additives). The emission measurements were carried out in each case for steady operating conditions (i.e., constant flue-gas temperature of approximately 175 °C at the boiler flue gas outlet after 1 h of operation) under full load conditions and over a period of approximately 3–4 h. After each combustion trial, the combustion plant was shut down completely for cleaning purposes, preparation of the following test setup and to ensure comparable operating conditions throughout the entire test series.

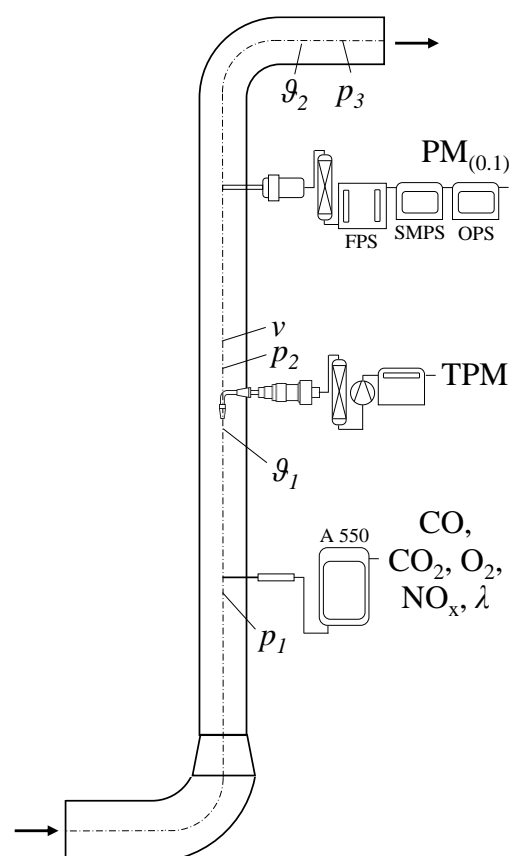


**Figure 2.** Schematic drawing of the measuring section of the small-scale combustion plant RHK-AK 30 (TPM: total particulate matter,  $PM_{(0.1)}$ : (ultrafine) particulate matter, CO: carbon monoxide,  $CO_2$ : carbon dioxide,  $O_2$ : oxygen,  $NO_x$ : nitrogen oxides,  $\lambda$ : excess air ratio,  $p_1$ – $p_3$ : pressure measurements,  $\vartheta_1$ – $\vartheta_2$ : temperature measurements,  $v$ : velocity measurement, FPS: fine particle sampler, SMPS: scanning mobility particle sizer, OPS: optical particle sizer).

## 2.4. Total Particulate Matter (TPM) Emissions

### 2.4.1. Gravimetric Determination

The TPM emissions were determined following a discontinuous, gravimetric measuring procedure according to DIN EN 13284-1 [68] and DVI 2066-1 [69]. For this purpose, a partial volume flow of the flue gas was sampled under isokinetic conditions at a repre-

representative point of the measuring section designed in accordance with DIN EN 15259 [67] (Figure 2). The sampling duration was 5 min. An out-stack filter unit (Paul Gothe GmbH, Bochum, Germany) was used as a sampling device. The sampling device was heated during the measurements (i.e., according to the flue-gas temperature) to avoid condensation effects that would distort the determination of the TPM emissions. Within this sampling device, the TPM contained in the partial volume flow of the flue gas was deposited during each measurement on a weighed quartz fiber flat filter. This filter has previously been heated in a laboratory drying oven (LUT 6050, Heraeus Holding GmbH, Hanau, Germany) at a temperature of 160 °C for 1 h and then cooled to room temperature for at least 8 h in a desiccator. After sampling, the loaded flat filters were heated, cooled, and weighed as before. In addition to the mass of the TPM on the filters, the mass of the TPM deposited in the front part of the sampling device was also attributed to the sampled partial volume flows of the flue gas. During each combustion trial (Table 1) of about three to four hours (i.e., both wood chips without and with additive), twelve flat filters ( $n_{total} = 72$ ) were used. Once stable operating conditions were reached, the TPM emissions were determined approximately every 15–20 min in order to be able to represent the emission behavior over the entire test duration. The TPM emissions are reported for dry flue gas under standard conditions (i.e.,  $p = 101,325$  Pa and  $T = 273.15$  K) and a reference oxygen concentration of 13 vol% in the flue gas. Once the gravimetric determination of the TPM emissions had been completed, the twelve flat filters per combustion trial (i.e., a total of six trials) were used proportionally to determine the chemical composition of the TPM emissions in the laboratory (i.e., by atomic absorption spectrometry (AAS) and ion chromatography (IC)).

#### 2.4.2. Chemical Composition

To determine the chemical composition of the TPM emissions as well as the corresponding K emissions, the loaded quartz fiber flat filters from the combustion trials were analyzed by atomic absorption spectrometry (AAS) and ion chromatography (IC). At least three flat filters for each combustion trial were treated according to DIN 22022-1 [70] with 12 mL aqua regia (i.e., three parts hydrochloric acid (32%): one part nitric acid (65%)) in a microwave digestion system (Multiwave GO Plus, Anton Paar Germany GmbH, Ostfildern-Scharnhausen, Germany) with temperatures up to 190 °C, a pressure of up to 20 bar, and a maximum power input of 1000 W for 35 min prior to the AAS measurements. The obtained solutions were analyzed according to DIN 22022-3 [71] in an air-acetylene or nitrous-acetylene flame of an atomic absorption spectrometer (contraAA 700, Analytik Jena GmbH+Co. KG, Jena, Germany) for the concentration of various inorganic elements (e.g., potassium (DIN 38406-13 [72]), sodium (DIN 38406-14 [73]), and calcium (DIN EN ISO 7980 [74])). For the IC measurements, at least three flat filters of each combustion trial were treated with demineralized water (i.e., suspended in 10 mL of demineralized water on a vibrating plate for 1 h). The resulting solutions were filtered (i.e., pore diameter of 45 µm) and analyzed for water-soluble components or dissolved anions (e.g., sulfate or chloride) by an ion chromatograph system (ICS-90, Dionex Softron GmbH, Germering, Germany) in accordance with DIN EN ISO 10304-1 [75].

#### 2.4.3. Particle Size Number Distribution

To analyze the particle size number distribution of the ultrafine fraction of the TPM emissions ( $PM_{0.1}$ ) for the different combustion trials, a partial volume flow of the flue gas was taken and accordingly diluted with compressed air of the same temperature by means of a fine particle sampler (FPS-4000, Dekati Ltd., Kangasala, Finland) at a representative point of the measuring section (Figure 2) according to DIN EN 15259 [67]. An identical dilution rate of approximately 1:100 was used for all six combustion trials. A combination of a scanning mobility particle sizer (NanoScan SMPS 3910, TSI GmbH, Aachen, Germany) and an optical particle sizer (OPS 3330, TSI GmbH, Aachen, Germany) was used to analyze the diluted volume flow in the size range from 10 nm to 10 µm. For standardization and evaluation of the data from both devices (i.e., SMPS and OPS), the multi-instrument

manager (MIM 2.0, TSI GmbH, Aachen, Germany) software was used [76]. For each combustion trial (Table 1), cumulative particle size number distributions ( $Q_0$ ) are reported as averages of thirty one-minute measurements.

### 2.5. Carbon Monoxide (CO) Emissions

The determination of the CO emissions took place every 10 s after stable operating conditions were reached (i.e., after approximately 1 h of heating the combustion plant and over a subsequent period of 3–4 h) via a flue-gas analyzer (A 550, Wöhler Technik GmbH, Bad Wünnenberg, Germany) within the measurement section (Figure 2). The CO emissions are determined using an electrochemical sensor. CO emissions are reported for flue gas on a dry reference base, under standard conditions (i.e.,  $p = 101,325$  Pa and  $T = 273.15$  K) and for an oxygen reference concentration of 13 vol%. As additional measured variables, the concentrations of carbon dioxide (i.e., calculated value), oxygen (i.e., determined electrochemically), and nitrogen oxides (i.e., determined electrochemically) in the flue gas as well as the excess air ratio ( $\lambda$ ) (i.e., calculated value) could also be determined by the device used.

### 2.6. Ashes

Five ash samples were taken at regular intervals (i.e., approximately every 40–45 min) for each combustion trial (Table 1) after a constant flue-gas temperature had been reached under full load conditions for the 33-kW combustion plant. Prior to further analyses, each individual ash sample was homogenized.

#### 2.6.1. Chemical Composition

The chemical composition of the ashes was analyzed due to general analysis samples (~100 mg) (DIN EN ISO 16967 [77] and DIN EN ISO 16968 [78]) using AAS (DIN 22022-1 [70] and DIN 22022-3 [71]) and IC (DIN EN ISO 10304-1 [75]) just as for the TPM flat filters (Section 2.4.2). All analyses (i.e., for each element within the AAS measurements and for each anion within the IC measurements) were performed as triplicates.

#### 2.6.2. Crystalline Phases

The crystalline phases of the ashes were also analyzed on the basis of general analysis samples (~1 g) by X-ray diffraction (XRD) (DIN EN 13925-1 [79] and DIN EN 13925-2 [80]). The ashes were ground and then placed on a sample carrier in preparation for the measurement. For this purpose, an X-ray diffractometer (D500, Siemens AG, Munich, Germany) was used (i.e., using Cu  $K\alpha$  radiation at 30 mA and 40 kV with step scanning (step width:  $0.05^\circ$ , step time: 1 s) in the range of  $20$ – $60^\circ$ ), while the resulting diffractograms were evaluated with respect to the occurrence of crystalline phases using an associated software (DIFFRAC<sup>plus</sup> EVA 11.0.0.3, Bruker Corporation, Billerica, MA, USA). The corresponding analyses were performed in triplicate.

## 3. Results and Discussion

In total, two non-additivated and four additivated wood-chip samples were produced and investigated in a 33-kW combustion plant. Each of these wood-chip samples or combustion trials has a corresponding denotation (Table 1) used in the following figures and tables (i.e., *without Additive*, *Kaolin*, *Anorthite*, *Aluminum hydroxide*, *Titanium dioxide*, and *ESP*).

### 3.1. Total Particulate Matter (TPM) Emissions

#### 3.1.1. Gravimetric Determination

The mean TPM emissions for the combustion of non-additivated wood chips (i.e., without and with ESP) and additivated wood chips (i.e., 1.0 wt%<sub>a.r.</sub> kaolin, anorthite, aluminum hydroxide or titanium dioxide) are summarized in Figure 3.

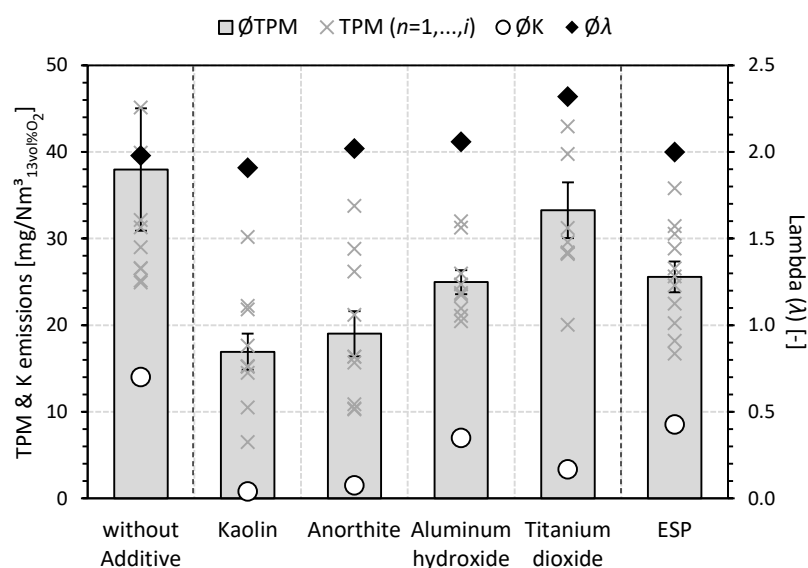


**Figure 3.** Mean total particulate matter (TPM) emissions (i.e., single values ( $n \leq 12$ )), mean potassium (K) emissions and mean excess air ratio ( $\lambda$ ) for combustion trials of non-additivated (without and with ESP) and additivated (1.0 wt%<sub>a.r.</sub> kaolin, anorthite, aluminum hydroxide or titanium dioxide) wood chips (a.r.: wood chips as received).

By using the ESP as a secondary PM mitigation measure, the TPM emissions can be reduced from 38 mg/Nm<sup>3</sup> to 26 mg/Nm<sup>3</sup> (−33%) compared to the reference case without an additive and without ESP (i.e., *without Additive*); this qualitative emission mitigation behavior of the ESP was to be expected. The relative reduction in TPM emissions through the use of the ESP as well as the absolute emission values show excellent agreement with the results of another study [53], which was carried out on the same combustion plant and also used pine wood chips as fuel. In this previous series of measurements, average TPM emissions of 36 mg/Nm<sup>3</sup> were determined for the reference case (i.e., without additives and without ESP) and 23 mg/Nm<sup>3</sup> for the utilization of the ESP under identical test conditions [53]. Thus, despite the lack of repetitions of the individual combustion trials within the scope of the present study (e.g., conducting *without Additive* or *ESP* twice), it can be assumed that the measured emission values are highly replicable and reproducible and, therefore, highly robust.

Figure 3 shows that a reduction in TPM emissions compared to the reference case (i.e., *without Additive*) can also be observed for all additives used. This result can be interpreted as empirical evidence for the basic transferability of the primary PM mitigation measure of (fuel) additivation to the fuel-type wood chips. Thus, assumptions from laboratory investigations [52,81] and other test series [49,53] regarding the additvability of wood chips can be proven or confirmed for systematic combustion trials in a small-scale combustion plant.

The present investigation also allows a direct comparison between fuel-related and secondary PM mitigation measures. Here, comparable TPM emissions of 25 mg/Nm<sup>3</sup> and 26 mg/Nm<sup>3</sup> can be achieved both by adding aluminum hydroxide to the wood chips and by using the ESP, respectively. For titanium dioxide, the TPM emissions are significantly higher (33 mg/Nm<sup>3</sup>). The achievable reduction of the TPM emissions compared to the reference case (*without Additive*) by aluminum hydroxide (−34%) and the ESP (−33%) can even be exceeded by the additives kaolin (−55%) and anorthite (−50%). These relative mitigation effects of kaolin and anorthite even exceed the TPM reduction (−44%) that Mack et al. found for the addition of 1.5 wt. %<sub>a.r.</sub> kaolin to poplar wood chips [49]. With values of 17 mg/Nm<sup>3</sup> (*Kaolin*) and 19 mg/Nm<sup>3</sup> (*Anorthite*), the mean TPM emissions are below the currently valid German legal threshold of 1. BImSchV (20 mg/Nm<sup>3</sup>) [51]; in an earlier study, the authors were already able to achieve mean TPM emissions of 23 mg/Nm<sup>3</sup> for

the additivation of pine wood chips with 0.5 wt%<sub>a.r.</sub> kaolin [53]. Thus, the operation of the small-scale combustion plant in conformity with the legal emission limits for PM emissions could be achieved exclusively by the additivation of the used solid biofuel (i.e., pine wood chips). Similar qualitative mitigation effects for aluminum-silicate-based additivation of solid wood fuels have already been demonstrated [20,47].

### 3.1.2. Chemical Composition

The chemical compositions of the TPM emissions for the combustion of non-additivated wood chips (i.e., *without Additive* and *ESP*) as well as additivated wood chips using kaolin, anorthite, aluminum hydroxide, or titanium dioxide are shown in Table 4. The derived K emissions (i.e., the mean concentration of K in the TPM emissions) are additionally presented in Figure 3.

**Table 4.** Chemical composition of total particulate matter (TPM) emissions for combustion trials of non-additivated (without and with ESP) and additivated (1.0 wt%<sub>a.r.</sub> kaolin, anorthite, aluminum hydroxide or titanium dioxide) wood chips (a.r.: wood chips as received, d.b.: dry TPM basis).

Parameter	Unit	Without Additive	Kaolin	Anorthite	Aluminum Hydroxide	Titanium Dioxide	ESP
Potassium (K)	wt% <sub>d.b.</sub>	36.9	4.9	8.0	28.1	10.1	33.4
Sodium (Na)	wt% <sub>d.b.</sub>	1.3	0.8	3.0	0.8	0.9	0.7
Calcium (Ca)	wt% <sub>d.b.</sub>	4.8	12.4	10.0	7.2	7.8	7.6
Magnesium (Mg)	wt% <sub>d.b.</sub>	<0.1	<0.1	0.2	0.3	0.2	0.2
Aluminum (Al)	wt% <sub>d.b.</sub>	<0.1	<0.1	<0.1	<0.1	<0.1	<0.1
Iron (Fe)	wt% <sub>d.b.</sub>	2.7	5.8	5.0	3.3	3.4	4.9
Zinc (Zn)	wt% <sub>d.b.</sub>	1.4	2.1	1.8	1.6	1.5	1.1
Sulfate (SO <sub>4</sub> <sup>2-</sup> )	wt% <sub>d.b.</sub>	41.7	7.7	21.2	42.7	10.0	30.1
Chloride (Cl <sup>-</sup> )	wt% <sub>d.b.</sub>	6.3	3.9	14.4	8.5	6.3	5.0
Not identified	wt% <sub>d.b.</sub>	4.9	62.3	36.5	7.5	59.7	17.0

For the reference case (*without Additive*), the TPM emissions mainly consist of the inorganic components K (36.9 wt%<sub>d.b.</sub>), sulfate (41.7 wt%<sub>d.b.</sub>), and chloride (6.3 wt%<sub>d.b.</sub>); this is also in good agreement with the previous study [53]. Together, these species form the volatile K compounds (i.e., K<sub>2</sub>SO<sub>4</sub> and KCl) that make up the majority of inorganic TPM emissions; i.e., particularly within the ultrafine particle fraction PM<sub>0.1</sub> [26]. This again emphasizes the correlation between the K originating from the solid biofuel used (Table 2) and the resulting release of gaseous K species (Table 4) as well as the subsequent formation of TPM emissions (Figure 3) during pure/untreated biomass combustion [14,15,82].

While the TPM emissions for the utilization of the ESP can be reduced by one-third compared to the reference case without additives and without ESP (i.e., *without Additive*; Figure 3), the proportions of K (33.4 wt%<sub>d.b.</sub>), sulfate (30.1 wt%<sub>d.b.</sub>), and chloride (5.0 wt%<sub>d.b.</sub>) in the corresponding (still released) TPM emissions, however, decrease only slightly. Consequently, the ESP does not result in a significant, chemically selective reduction of certain TPM species (e.g., K compounds), but rather, due to the physical mode of action [8,9], in a (uniform) TPM mitigation throughout the entire particle size range [83]. Assuming a particularly efficient reduction effect of the ESP with respect to PM emissions (i.e., particle diameter ( $d_p \leq 10 \mu\text{m}$ )), the slight increase in the relative proportion of calcium (7.6 wt%<sub>d.b.</sub>) and not identified species (17.0 wt%<sub>d.b.</sub>) of the TPM emissions could possibly be attributed to coarse fly ash particles (e.g.,  $10 \mu\text{m} \leq d_p \leq 200 \mu\text{m}$ ) entrained by the flue gas during the combustion process (e.g., calcium oxide (CaO) or calcium carbonate (CaCO<sub>3</sub>) [84]).

Unlike for the ESP, the relative K proportions of the TPM emissions (Table 4) and thus the K emissions (Figure 3) can be reduced by all additives investigated (i.e., analogous to the preliminary laboratory-scale investigations [52]). This behavior provides further evidence for the effectiveness of (fuel) additivation of wood chips; i.e., reduced K-related

TPM emissions by high-temperature stable K incorporation into the ash. Due to the significant reduced K emissions (i.e., *Kaolin* (−94%), *Anorthite* (−89%), *Aluminum hydroxide* (−50%), and *Titanium dioxide* (−76%)), the relative composition of the TPM emissions for the additivated wood chips changes; i.e., the proportions of calcium and not identified components of the TPM emissions (i.e., elements/species [e.g., oxides, inorganic/organic carbon] that cannot be determined by the analytical methods used) increase. A dark discoloration due to the separated TPM emissions could be determined for all flat filters examined, which supports the hypothesis that a proportion of the TPM—that cannot be quantified analytically here (i.e., determination by ashing the filters was not successful)—is probably attributed to organic or carbonaceous compounds. Nevertheless, the reduced K emissions could result in further advantages in addition to the mitigated TPM emissions. For example, the presence of alkali compounds in the flue gas can lead to the formation and growth of sticky deposits on heat exchanger surfaces in combustion systems, which can reduce heat transfer or promote corrosion. Furthermore, K compounds in the flue gas or as part of the TPM emissions can act as catalyst poisons in DeNO<sub>x</sub> units (i.e., selective catalytic reduction (SCR)) of large-scale combustion plants; this shortens the lifetime and increases operating costs.

Based on the results in Figure 3 and Table 4, the combined use of primary, fuel-related mitigation measures (e.g., fuel additivation) and secondary (e.g., ESP) mitigation measures should be investigated in more detailed to be able to reliably comply with existing emission limits and, if possible, to be able to exploit further advantages.

### 3.1.3. Particle Size Number Distribution

Figure 4 shows the particle size number distributions and the corresponding cumulative distributions for the PM emissions within the combustion trials performed (Table 1). The reference case *without Additive* shows a typical unimodal characteristic for the particle size number distribution (modal value 55 nm) [2,85,86], while 91% of the PM emissions can be assigned to the ultrafine particle fraction PM<sub>0.1</sub> (i.e., these PM particles have a particle diameter  $d_p \leq 100$  nm) on the basis of the cumulative particle size number distribution.

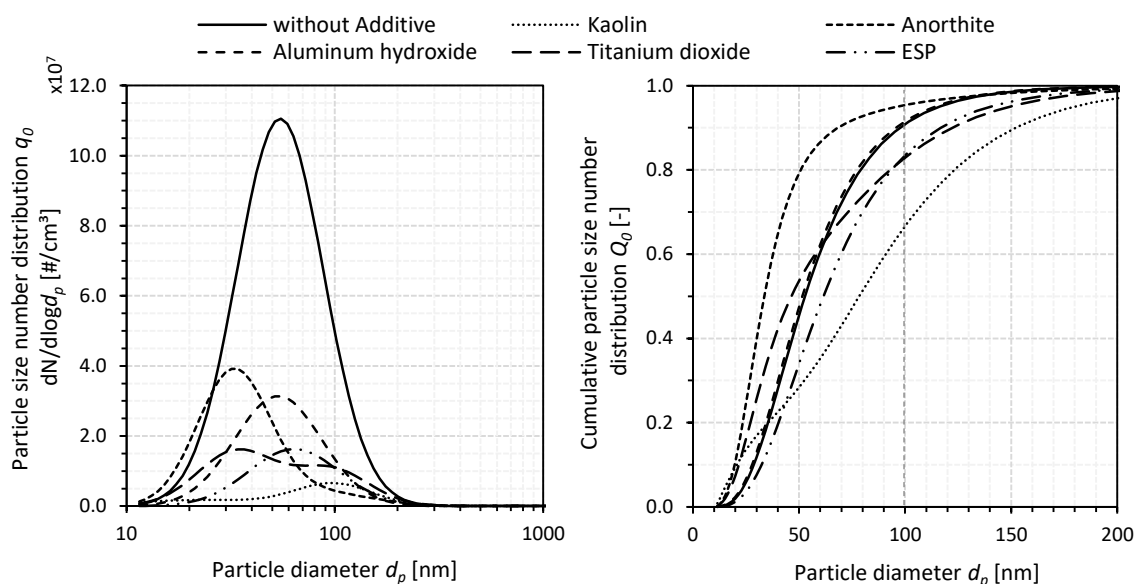


**Figure 4.** Particle size number distribution (left) and cumulative particle size number distribution (right) of the particulate matter (PM) emissions for combustion trials of non-additivated (without and with ESP) and additivated (1.0 wt%<sub>a.r.</sub> kaolin, anorthite, aluminum hydroxide or titanium dioxide) wood chips ( $q_0/Q_0$ : density/cumulative distribution of the quantity type number determined by mobility and optical analysis, a.r.: wood chips as received).

Compared to the reference case, the absolute number of PM particles can be significantly reduced for all investigated additives (i.e., kaolin, anorthite, aluminum hydroxide, and titanium dioxide) as well as for the ESP [14]. Figure 4 shows that the characteristics of the particle size number distributions for the additives and ESP differ in some cases. For example, *Aluminum hydroxide* (modal value 53 nm) and *ESP* (modal value 63 nm) show typical unimodal distributions, while a left-skewed unimodal characteristic is obtained for *Kaolin* (modal value 94 nm), and a right-skewed unimodal characteristic for *Anorthite* (modal value 32 nm). The particle size number distribution for *Titanium dioxide* (modal values 34 nm and 83 nm), on the other hand, resembles a bimodal pattern.

Consequently, there are also different results regarding the share of the PM<sub>0.1</sub> fraction in the PM emissions (i.e., cumulative particle size number distribution (Figure 4)). Although PM<sub>0.1</sub> emissions contribute only slightly to the total particle mass, PM<sub>0.1</sub> particles can be particularly relevant to health due to their high mobility within the human body as well as their large specific surface area [87].

While the share of the PM<sub>0.1</sub> fraction within the PM emissions does not change for the additive aluminum hydroxide (92%) compared to the reference case (91%), a slight relative increase in the number of PM<sub>0.1</sub> particles in the PM emissions can be observed while using anorthite (95%). An analogous behavior for the additive anorthite could already be shown for kaolin; however, primarily agricultural fuels were investigated [53,88,89]. In contrast to the literature, the addition of kaolin to the wood chips in these measurements does not show an increased share of ultrafine particles in the PM emissions or a shift of the maximum of the particle size number distribution to smaller particle diameters [47]. Instead, the share of the PM<sub>0.1</sub> fraction within the PM emissions is even lower for *Kaolin* (67%) than for *Titanium dioxide* (83%) or *ESP* (83%). Thus, the aluminum-silicate-based (fuel) addition of wood chips can result not only in TPM emissions in compliance with the legal emission limits (Figure 3) but also in a reduced relative share of PM<sub>0.1</sub> particles within the (still emitted) PM emissions.

### 3.2. Carbon Monoxide (CO) Emissions

Figure 5 summarizes the mean CO emissions for the combustion trials performed. The individual CO emission curves over the test periods are shown together with the ash sampling intervals in Figure 6.

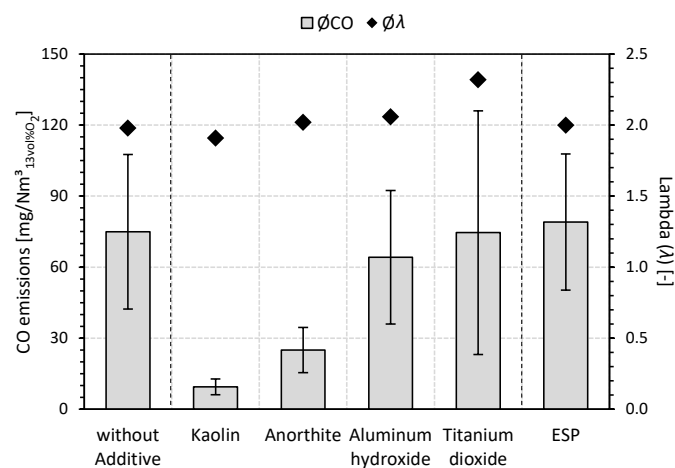


**Figure 5.** Mean carbon monoxide (CO) emissions and mean excess air ratio ( $\lambda$ ) for combustion trials of non-additivated (without and with ESP) and additivated (1.0 wt%<sub>a.r.</sub> kaolin, anorthite, aluminum hydroxide or titanium dioxide) wood chips (a.r.: wood chips as received).

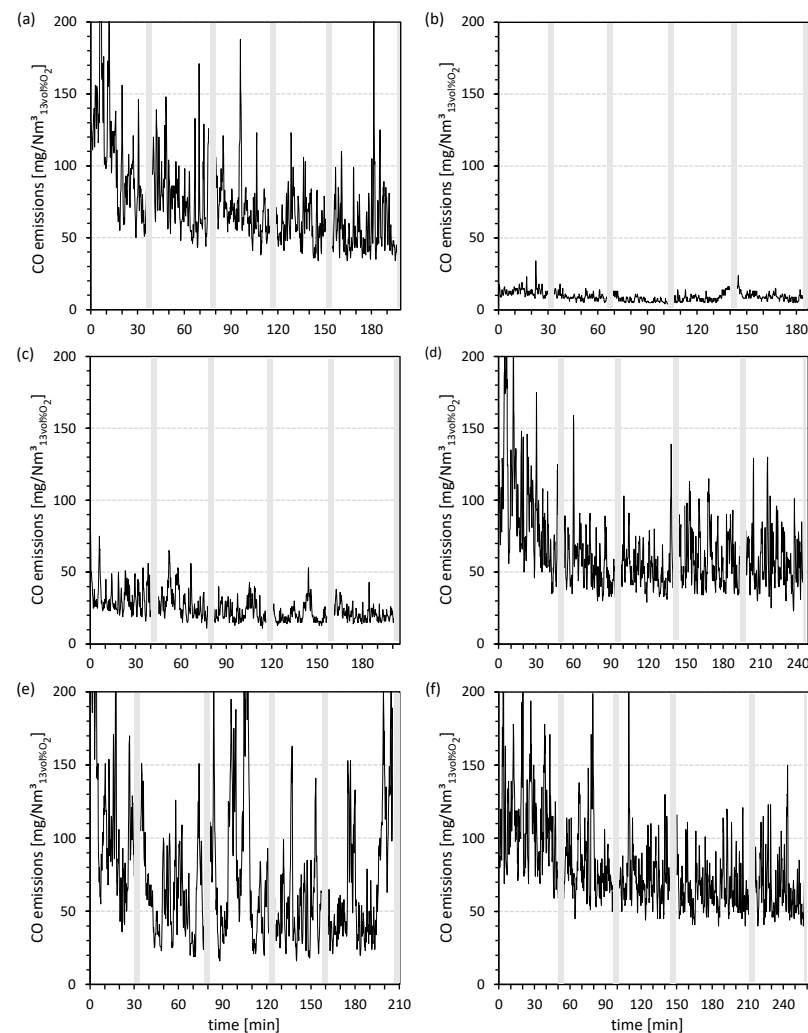


**Figure 6.** Carbon monoxide (CO) emissions and ash sampling intervals (gray areas) for the wood-chip combustion trials: (a) without additives, (b) 1.0 wt%<sub>a.r.</sub> kaolin, (c) 1.0 wt%<sub>a.r.</sub> anorthite, (d) 1.0 wt%<sub>a.r.</sub> aluminum hydroxide, (e) 1.0 wt%<sub>a.r.</sub> titanium dioxide and (f) with ESP (a.r.: wood chips as received).

As expected, the mean CO emissions for the two non-additivated cases (i.e., *without Additive* (75 mg/Nm<sup>3</sup>) and *ESP* (79 mg/Nm<sup>3</sup>) do not differ due to the mitigation measure used; nevertheless, both are well below the legal CO emission limit of 400 mg/Nm<sup>3</sup> [51]. Based on these two values (Figure 5), good replicability of the determined emission data can be derived since comparable emission levels and behavior can be achieved across different combustion trials (Figure 6).

The additive titanium dioxide shows mean CO emissions (75 mg/Nm<sup>3</sup>) comparable to the two non-additivated cases. Figure 6 shows, however, that the CO emissions for *Titanium dioxide* fluctuate significantly more over the duration of the combustion trial; high CO peaks occur repeatedly. Compared to that, the other additives (i.e., kaolin (−87%), anorthite (−67%), and aluminum hydroxide (−14%)) show a reduction in mean CO emissions compared to the reference cases *without Additive* and *ESP*. A similar effect has already been observed for kaolin and kaolinite (e.g., Mack et al. report a reduction in CO emissions from 886 mg/Nm<sup>3</sup> to 47 mg/Nm<sup>3</sup> (−95%) for the use of 1.5 wt%<sub>a.r.</sub> in the small-scale combustion of poplar wood chips) [47,49]. This observed CO mitigation has so far been associated with possible physical and/or chemical (catalytic) effects of the kaolin/kaolinite (e.g., favored CO oxidation by changing the ash structure due to additivation or catalytic activity of the additive regarding oxidation reaction) [47,49]. But it is known that the demineralization of biomass by washing also leads to significantly reduced CO emissions during combustion.

In this context, water-soluble K (e.g., KCl) in particular shows high extraction rates of 50 up to 100%. Here a dependence of the K level during the combustion and the emitted CO emissions (i.e., absence of leachable K species and mitigated CO levels) seem to be plausible [90].

Thus, an approach that has received little attention so far relates to (moist) CO oxidation (e.g., biomass combustion processes) in the presence of gaseous K species [91–94]. Within a combustion unit, CO oxidation is predominately controlled by the availability of free radicals (e.g., hydroxyl radicals) within the gas phase [91,94]. However, gaseous KCl and KOH, in particular, can lead to a recombination of the corresponding radicals by gas-phase reactions at high temperatures (i.e., 600 up to 1200 °C), which, in turn, inhibits CO oxidation [93]. Consequently, the fewer of these K species that are available for the indicated recombination reactions (e.g., by heterogeneous gas-solid reactions with additives), results in a decrease in (inorganic) TPM emissions and CO oxidation might happen more unhindered [95].

This behavior can be confirmed in particular for the additives kaolin, anorthite, and aluminum hydroxide. While the achievable reductions in both TPM and K emissions (Figure 3) continue to increase from aluminum hydroxide (i.e., TPM (−34%) and K (−50%)), through anorthite (i.e., TPM (−50%) and K (−89%)) to kaolin (i.e., TPM (−55 %) and K (−94 %)) compared with the reference case *without Additive*, analogous behavior is also seen for the CO emissions. These results show good agreement with a comparable study investigating the influence of aluminum-(silicate-)based fuel additivation for small-scale wood-pellet combustion [96]. In comparison, although the ESP also reduces the TPM emissions and consequently the K emissions proportionally, the flue-gas temperatures at the ESP location are only about 200 °C (i.e., as expected, the secondary mitigation measure does not influence the components within the reactive gas phase in the course of CO oxidation localized clearly further upstream within the flue-gas path). Mitigation in K emissions (−76%) can also be achieved with titanium dioxide, but neither TPM emissions nor CO emissions are significantly reduced, which could be an indication of the phenomenologically different behavior of titanium dioxide compared with the other additives (e.g., titanium dioxide as a catalyst support material in other applications).

As NO<sub>x</sub> emissions were also determined during the analysis of CO emissions in the present study, the corresponding findings should also be briefly examined here. Studies in the literature suggest that fuel additivation can lead to an increase in NO<sub>x</sub> emissions [49]. In the course of the combustion trials carried out here, however, mean NO<sub>x</sub> emissions of 110 mg/Nm<sup>3</sup> (*without Additive*), 115 mg/Nm<sup>3</sup> (*Kaolin*), 113 mg/Nm<sup>3</sup> (*Anorthite*), 113 mg/Nm<sup>3</sup> (*Aluminum hydroxide*), 115 mg/Nm<sup>3</sup> (*Titanium dioxide*), and 110 mg/Nm<sup>3</sup> (*ESP*) were found; the standard deviation in all cases is ≤4 mg/Nm<sup>3</sup>. Thus, no significant increase in NO<sub>x</sub> emissions can be determined as a result of the addition of the additives.

### 3.3. Ashes

#### 3.3.1. Chemical Composition

The chemical composition of the ashes for all combustion trials (Table 1) is shown in Table 5. The results for the chemical composition of the ashes of the non-additivated wood chips (i.e., *without Additive* and *ESP*) show, as expected, good agreement and replicability. Due to the additive addition, the absolute amount of ash produced increases resulting in a decrease in the relative proportion of the corresponding ash components (e.g., calcium, magnesium); given that these are not additionally introduced by the utilized additives (i.e., kaolin, anorthite, aluminum hydroxide, and titanium dioxide).

**Table 5.** Chemical composition of the ashes for combustion trials of non-additivated (without and with ESP) and additivated (1.0 wt%<sub>a.r.</sub> kaolin, anorthite, aluminum hydroxide, or titanium dioxide) wood chips (a.r.: wood chips as received, d.b.: dry ash basis).

Parameter	Unit	Without Additive	Kaolin	Anorthite	Aluminum Hydroxide	Titanium Dioxide	ESP
Potassium (K)	wt% <sub>d.b.</sub>	13.2	3.7	3.5	4.6	3.7	10.4
Sodium (Na)	wt% <sub>d.b.</sub>	0.1	0.1	2.4	0.3	0.3	0.3
Calcium (Ca)	wt% <sub>d.b.</sub>	23.3	5.6	8.5	8.3	6.4	25.6
Magnesium (Mg)	wt% <sub>d.b.</sub>	5.4	1.6	1.6	1.8	1.3	5.9
Aluminum (Al)	wt% <sub>d.b.</sub>	2.5	11.7	8.8	28.2	1.4	4.2
Iron (Fe)	wt% <sub>d.b.</sub>	0.6	0.7	1.2	0.4	0.5	1.1
Zinc (Zn)	wt% <sub>d.b.</sub>	<0.1	<0.1	<0.1	<0.1	<0.1	<0.1
Sulfate (SO <sub>4</sub> <sup>2-</sup> )	wt% <sub>d.b.</sub>	1.5	0.8	0.6	0.7	0.6	1.5
Chloride (Cl <sup>-</sup> )	wt% <sub>d.b.</sub>	<0.1	<0.1	<0.1	<0.1	<0.1	<0.1
Not identified	wt% <sub>d.b.</sub>	53.3	75.8	73.4	55.6	85.9	51.0

Consequently, for all additives, a reduction in the relative proportion of the non-volatile alkaline earth element calcium compared with the non-additivated ashes can be observed, with the largest proportion using anorthite (8.5 wt%<sub>d.b.</sub>); since here, in addition to the calcium originating from the wood chips, additional amounts of this element are introduced into the ash via the additive itself. For anorthite, the chemical composition of the additive also leads to an increase in the absolute amount of aluminum and silicon in the associated ash, which is necessary for the formation of high-temperature stable K-aluminum silicates. With a value of 8.8 wt%<sub>d.b.</sub>, the relative proportion of aluminum in the ash of *Anorthite* is, nevertheless, lower than for the aluminum-silicate-based additivation using kaolin (11.7 wt%<sub>d.b.</sub>) and significantly lower than for the aluminum-based additivation using aluminum hydroxide (28.2 wt%<sub>d.b.</sub>). Accordingly, adding titanium dioxide to the wood chips results in a decrease in the amount of aluminum in the ash.

Finally, for the highly volatile, ash- and PM-forming K, the (fuel) additivation results in relative proportions in the ashes of 3.7 wt%<sub>d.b.</sub> (*Kaolin*), 3.5 wt%<sub>d.b.</sub> (*Anorthite*), 4.6 wt%<sub>d.b.</sub> (*Aluminum hydroxide*), and 3.7 wt%<sub>d.b.</sub> (*Titanium dioxide*), which are significantly lower than the corresponding values for the non-additivated wood chips (i.e., *without Additive* and *ESP*). However, again, the addition of additive increases the absolute amount of ash resulting in a dilution effect and consequently in a reduction of the relative proportion of specific ash components [14,15]. Thus, the reduced relative proportion of K in the ashes of the additivated wood chips is by no means in fundamental contradiction to the successful ash incorporation of the alkali element by the additives investigated.

The not-identified portions of the ashes may be partly due to unburned fuel particles and/or binding partners (e.g., oxygen, carbon, and silicon) of the elements analyzed in Table 5. A qualitative indication of the presence of corresponding compounds (e.g., oxides, carbonates, or silicates) is provided by the crystalline phase analysis shown below, which, however, does not allow any statement to be made about potentially present amorphous ash components.

### 3.3.2. Crystalline Phases

Table 6 shows the identified crystalline phases in the ashes for the combustion of non-additivated (i.e., without and with ESP) and additivated (i.e., 1.0 wt%<sub>a.r.</sub> kaolin, anorthite, aluminum hydroxide, and titanium dioxide) wood chips. In the ashes of the non-additivated wood chips, the crystalline compounds K sulfate (K<sub>2</sub>SO<sub>4</sub>) and K calcium carbonate (K<sub>2</sub>Ca(CO<sub>3</sub>)<sub>2</sub>) are present. These compounds could also be identified in the corresponding ashes of pure wood chips in the course of the laboratory investigation of the ashes formed at different temperatures (e.g., 550 °C and 1100 °C) [52]. Both compounds show moderate melting temperatures (i.e., K<sub>2</sub>SO<sub>4</sub> (1069 °C) and K<sub>2</sub>Ca(CO<sub>3</sub>)<sub>2</sub> (815 °C)) and,

when exposed to thermal treatment during combustion, might lead to gaseous release of K with subsequent (inorganic) TPM formation [24,25,97].

**Table 6.** Crystalline phases of the ashes for combustion trials of non-additivated (without and with ESP) and additivated (1.0 wt%<sub>a.r.</sub> kaolin, anorthite, aluminum hydroxide, or titanium dioxide) wood chips (a.r.: wood chips as received).

Parameter	Without Additive	Kaolin	Anorthite	Aluminum Hydroxide	Titanium Dioxide	ESP
K <sub>2</sub> SO <sub>4</sub>	x					x
K <sub>2</sub> Ca(CO <sub>3</sub> ) <sub>2</sub>	x					x
KAlSiO <sub>4</sub>		x				
KAlSi <sub>2</sub> O <sub>6</sub>			x			
KAlSi <sub>3</sub> O <sub>8</sub>		x	x	x		
KTi <sub>8</sub> O <sub>16</sub>					x	
K <sub>2</sub> TiO <sub>3</sub>					x	
K <sub>2</sub> Ti <sub>6</sub> O <sub>13</sub>					x	
K <sub>2</sub> TiSi <sub>6</sub> O <sub>15</sub>					x	
SiO <sub>2</sub>		x	x			
Al <sub>2</sub> O <sub>3</sub>				x		
CaO	x					x
CaCO <sub>3</sub>	x	x	x	x		x
MgO	x			x		x
TiO <sub>2</sub>					x	
Al <sub>6</sub> Si <sub>2</sub> O <sub>13</sub>		x				
CaAl <sub>2</sub> Si <sub>2</sub> O <sub>8</sub>			x			
Ca <sub>3</sub> Al <sub>2</sub> O <sub>6</sub>				x		
CaTiO <sub>3</sub>					x	

For the additivated of the wood chips using kaolin, analogous to the results of the laboratory investigation [52], high-temperature stable K aluminum silicates in the form of kalsilite (KAlSiO<sub>4</sub>) and orthoclase/microcline (KAlSi<sub>3</sub>O<sub>8</sub>), respectively, can be identified in the ashes. These K compounds can be understood as qualitative evidence for a reaction between kaolin and the K originating from the wood chips. Following this argumentation, the reduction in K emissions and, based on this, the reduction in TPM emissions (Figure 3) can clearly be attributed to the addition of the aluminum-silicate-based additive. The presence of the aluminum silicate Al<sub>6</sub>Si<sub>2</sub>O<sub>13</sub> for *Kaolin* can be interpreted as an indicator for unreacted additive or for an oversupply of the additive with respect to the desired reaction; i.e., K aluminum silicate formation. Thus, it can be assumed, that a further increase in the additive content (i.e., >1.0 wt%<sub>a.r.</sub> kaolin) is unlikely to lead to an additional increase in the high-temperature stable ash incorporation of K by kaolin; which also seems rather plausible in view of the already achieved K emission mitigation (−94%).

A qualitatively similar behavior can also be derived for anorthite based on the results of the crystalline phase analysis (Table 6). Here, high-temperature stable K aluminum silicates can also be identified in the ash with leucite (KAlSi<sub>2</sub>O<sub>6</sub>) and orthoclase/microcline (KAlSi<sub>3</sub>O<sub>8</sub>). Similar to *Kaolin*, unreacted additive (i.e., CaAl<sub>2</sub>Si<sub>2</sub>O<sub>8</sub>) can be detected for *Anorthite*. Hence, also for the calcium- and aluminum-silicate-based additive, taking into account the determined mitigation of the K emissions (−89%), it cannot be assumed that a further increase of the added additive amount (>1.0 wt%<sub>a.r.</sub>) will lead to a significant increase of the reduction effect.

Subsequently, the results for the additivated of the wood chips with aluminum hydroxide show the presence of orthoclase/microcline (KAlSi<sub>3</sub>O<sub>8</sub>), but also e.g., aluminum oxide (Al<sub>2</sub>O<sub>3</sub>) and calcium aluminum oxide (Ca<sub>3</sub>Al<sub>2</sub>O<sub>6</sub>), in the corresponding ash. While the addition of aluminum hydroxide solely introduces additional aluminum, it seems obvious that the formation of K aluminum silicates takes place with the aid of reactive silicon from the wood chips themselves. At the same time, this may result in limited reactivity if the required silicon is not available in sufficient quantity to completely incorporate K into

the ash. With an average reduction in K emissions of 50% and the presence of unreacted additive in the form of aluminum oxide ( $\text{Al}_2\text{O}_3$ ) in the ash for *Aluminum hydroxide*, it seems plausible to assume that silicon does indeed have a limiting influence here on the achievable mitigation effect of the merely aluminum-based additivation.

Although unreacted additive ( $\text{TiO}_2$ ) can also be detected in the ash for *Titanium dioxide*, unlike for kaolin and anorthite, an increased reduction in K emissions based on a corresponding value of 76% for the combustion trials by increasing the additive content does not seem entirely improbable. As expected, i.e., considering the results of the preliminary laboratory investigations [52], the high-temperature stable ash incorporation of K takes place primarily in the form of K titanates (e.g.,  $\text{K}_2\text{TiO}_3$  or  $\text{K}_2\text{Ti}_6\text{O}_{13}$ ). This demonstrably results in the essential difference from the other investigated additives.

#### 4. Conclusions

The main findings from the combustion trials carried out in the course of the present study can be summarized as follows.

- The transferability of (fuel) additivation of wood chips for not exclusively aluminum-silicate-based additives (e.g., kaolin or kaolinite [49,53]) could be demonstrated for a conventional small-scale combustion plant (33 kW). For all investigated additives (i.e., kaolin, anorthite, aluminum hydroxide, and titanium dioxide), a reduction of the mean TPM emissions could be observed during the combustion of additivated wood chips compared to the reference case without additives and without ESP.
- In agreement with a preliminary laboratory study [52], titanium dioxide showed the lowest reduction in TPM emissions (−12%) among the additives considered. The formation of high-temperature stable K titanates (e.g.,  $\text{K}_2\text{TiO}_3$  or  $\text{K}_2\text{Ti}_6\text{O}_{13}$ ) determined during the laboratory investigation [52] can also be qualitatively confirmed for the practical scale and used as a reason for the mitigation of K emissions (−76%).
- The reduction of the absolute mean TPM emissions by the use of aluminum hydroxide (−34%) is slightly behind the achievable effects by kaolin (−55%) and anorthite (−50%); however, compared to the non-additivated reference case, it leads to a comparable emission level as the ESP ( $26 \text{ mg}/\text{Nm}^3$ ).
- With reductions in mean K emissions of 94% and 89% compared to the reference case without additives and without ESP, respectively, the (fuel) additivation of the wood chips with  $1.0 \text{ wt}\%_{\text{a.r.}}$  kaolin or anorthite achieved the strongest effects. This is due to the formation of high-temperature stable K aluminum silicates (e.g., kalsilite ( $\text{KAlSiO}_4$ ), leucite ( $\text{KAlSi}_2\text{O}_6$ ), and orthoclase/microcline ( $\text{KAlSi}_3\text{O}_8$ )) in the associated ashes with mean emission levels of  $17 \text{ mg}/\text{Nm}^3$  (kaolin) and  $19 \text{ mg}/\text{Nm}^3$  (anorthite). Thus, for example, the German legal TPM emission limit of  $20 \text{ mg}/\text{Nm}^3$  [51] can be met. Thus, aluminum-silicate-based or calcium- and aluminum-silicate-based (fuel) additivation not only exceeds the reduction effect of the secondary mitigation measure in the form of the ESP but can also enable a plant operation that, in principle, does not require the use of a secondary mitigation measure. Nevertheless, the combined use of additivation as a primary fuel-related TPM mitigation measure and ESP as a secondary TPM mitigation measure appears to be very desirable in order to be able to exploit additional reduction potentials. In addition, the statement [52] can be underlined that a sole focus on kaolin or kaolinite as a promising additive does not necessarily appear to be justifiable against the background of the experimental results from the small-scale combustion plant considered with regard to anorthite.
- The (fuel) additivation of the wood chips with kaolin and the use of the ESP resulted in a shift of the particle size number distribution to larger particle diameters compared to the non-additivated reference case without ESP. For both mitigation measures, a reduction of the share of the ultrafine particle fraction ( $\text{PM}_{0.1}$ ) in the associated PM emissions was also detectable. Hence, the wood chips additivated with  $1.0 \text{ wt}\%_{\text{a.r.}}$  kaolin showed the largest simultaneous reduction of TPM, K, and  $\text{PM}_{0.1}$  emissions

for the investigated mitigation measures (i.e., (fuel) additivation depending on the additive type as well as ESP).

- In addition to the aluminum-silicate-based additivation of the wood chips with kaolin [49,53], the use of the calcium- and aluminum-silicate-based additive anorthite also leads to a significant decrease in the mean CO emissions (i.e., kaolin (−87%) and anorthite (−67%)) compared to the combustion of non-additivated wood chips as well as compared to the (fuel) additivation with titanium dioxide. With regard to the chemical composition of the additives used (e.g., kaolin, anorthite, and aluminum hydroxide), it can be assumed that the presence and reactive availability of aluminum and/or silicon as components of the additives could lead to a decrease in CO emissions (e.g., by influencing the (moist) CO oxidation due to the incorporation of the gaseous K species KOH and KCl into the ash). Despite the relatively strong reduction of K emissions (−76%) due to the use of titanium dioxide, neither the TPM nor the CO emissions can be significantly reduced by this additive, which highlights the phenomenologically deviating behavior of titanium dioxide compared to the other additives.

**Author Contributions:** C.G.: Conceptualization, Methodology, Investigation, Formal analysis, Validation, Visualization, Writing—Original Draft T.S.: Visualization, Formal analysis, Writing—Original Draft V.W.: Investigation, Formal analysis, Validation M.K.: Supervision, Project administration, Funding acquisition, Writing—Review and Editing. All authors have read and agreed to the published version of the manuscript.

**Funding:** This work was supported by the German Federal Environmental Foundation (Deutsche Bundesstiftung Umwelt, DBU) under grant number 32975/02. Publishing fees are supported by the Funding Program Open Access Publishing of Hamburg University of Technology (TUHH).

**Data Availability Statement:** The data presented in this study are available on request from the corresponding author.

**Acknowledgments:** We thank Christian Taraschewski and Natalie Mayer for their assistance with the sample analyses during the performed investigations.

**Conflicts of Interest:** The authors declare no conflicts of interest.

## References

1. Vicente, E.D.; Alves, C.A. An overview of particulate emissions from residential biomass combustion. *Atmos. Res.* **2018**, *199*, 159–185. [[CrossRef](#)]
2. Obaidullah, M.; Bram, S.; Verma, V.K.; de Ruyck, J. A Review on Particle Emissions from Small Scale Biomass Combustion. *Int. J. Renew. Energy Res. (IJRER)* **2012**, *2*, 147–159.
3. Tissari, J.; Sippula, O.; Kouki, J.; Vuorio, K.; Jokiniemi, J. Fine Particle and Gas Emissions from the Combustion of Agricultural Fuels Fired in a 20 kW Burner. *Energy Fuels* **2008**, *22*, 2033–2042. [[CrossRef](#)]
4. Schmidl, C.; Luisser, M.; Padouvas, E.; Lasselsberger, L.; Rzaca, M.; Ramirez-Santa Cruz, C.; Handler, M.; Peng, G.; Bauer, H.; Puxbaum, H. Particulate and gaseous emissions from manually and automatically fired small scale combustion systems. *Atmos. Environ.* **2011**, *45*, 7443–7454. [[CrossRef](#)]
5. McDonald, J.D.; Zielinska, B.; Fujita, E.M.; Sagebiel, J.C.; Chow, J.C.; Watson, J.G. Fine Particle and Gaseous Emission Rates from Residential Wood Combustion. *Environ. Sci. Technol.* **2000**, *34*, 2080–2091. [[CrossRef](#)]
6. Höfer, I.; Kaltschmitt, M.; Beckendorff, A. Emissions from solid biofuel combustion, Pollutant formation and control options. In *Encyclopedia of Sustainability Science and Technology*; Meyers, R.A., Ed.; Springer: New York, NY, USA, 2017.
7. Naeher, L.P.; Brauer, M.; Lipsett, M.; Zelikoff, J.T.; Simpson, C.D.; Koenig, J.Q.; Smith, K.R. Woodsmoke health effects: A review. *Inhal. Toxicol.* **2007**, *19*, 67–106. [[CrossRef](#)]
8. Singh, R.; Shukla, A. A review on methods of flue gas cleaning from combustion of biomass. *Renew. Sustain. Energy Rev.* **2014**, *29*, 854–864. [[CrossRef](#)]
9. Lim, M.T.; Phan, A.; Roddy, D.; Harvey, A. Technologies for measurement and mitigation of particulate emissions from domestic combustion of biomass: A review. *Renew. Sustain. Energy Rev.* **2015**, *49*, 574–584. [[CrossRef](#)]
10. Obernberger, I.; Brunner, T.; Mandl, C.; Kerschbaum, M.; Svetlik, T. Strategies and technologies towards zero emission biomass combustion by primary measures. *Energy Procedia* **2017**, *120*, 681–688. [[CrossRef](#)]
11. Lamberg, H.; Sippula, O.; Tissari, J.; Jokiniemi, J. Effects of Air Staging and Load on Fine-Particle and Gaseous Emissions from a Small-Scale Pellet Boiler. *Energy Fuels* **2011**, *25*, 4952–4960. [[CrossRef](#)]

12. Gehrig, M.; Jaeger, D.; Pelz, S.K.; Weissinger, A.; Groll, A.; Thorwarth, H.; Haslinger, W. Influence of firebed temperature on inorganic particle emissions in a residential wood pellet boiler. *Atmos. Environ.* **2016**, *136*, 61–67. [[CrossRef](#)]
13. Gollmer, C.; Höfer, I.; Kaltschmitt, M. Additives as a fuel-oriented measure to mitigate inorganic particulate matter (PM) emissions during small-scale combustion of solid biofuels. *Biomass Convers. Biorefinery* **2019**, *9*, 3–20. [[CrossRef](#)]
14. Míguez, J.L.; Porteiro, J.; Behrendt, F.; Blanco, D.; Patiño, D.; Dieguez-Alonso, A. Review of the use of additives to mitigate operational problems associated with the combustion of biomass with high content in ash-forming species. *Renew. Sustain. Energy Rev.* **2021**, *141*, 110502. [[CrossRef](#)]
15. Wang, L.; Hustad, J.E.; Skreiberg, Ø.; Skjevraak, G.; Grønli, M. A Critical Review on Additives to Reduce Ash Related Operation Problems in Biomass Combustion Applications. *Energy Procedia* **2012**, *20*, 20–29. [[CrossRef](#)]
16. Pollex, A.; Zeng, T.; Khalsa, J.; Erler, U.; Schmersahl, R.; Schön, C.; Kuptz, D.; Lenz, V.; Nelles, M. Content of potassium and other aerosol forming elements in commercially available wood pellet batches. *Fuel* **2018**, *232*, 384–394. [[CrossRef](#)]
17. Sippula, O.; Hytönen, K.; Tissari, J.; Raunemaa, T.; Jokiniemi, J. Effect of Wood Fuel on the Emissions from a Top-Feed Pellet Stove. *Energy Fuels* **2007**, *21*, 1151–1160. [[CrossRef](#)]
18. Lamberg, H.; Tissari, J.; Jokiniemi, J.; Sippula, O. Fine Particle and Gaseous Emissions from a Small-Scale Boiler Fueled by Pellets of Various Raw Materials. *Energy Fuels* **2013**, *27*, 7044–7053. [[CrossRef](#)]
19. van Lith, S.C.; Jensen, P.A.; Frandsen, F.J.; Glarborg, P. Release to the Gas Phase of Inorganic Elements during Wood Combustion. Part 2: Influence of Fuel Composition. *Energy Fuels* **2008**, *22*, 1598–1609. [[CrossRef](#)]
20. Gehrig, M.; Wöhler, M.; Pelz, S.; Steinbrink, J.; Thorwarth, H. Kaolin as additive in wood pellet combustion with several mixtures of spruce and short-rotation-coppice willow and its influence on emissions and ashes. *Fuel* **2019**, *235*, 610–616. [[CrossRef](#)]
21. van Lith, S.C.; Alonso-Ramírez, V.; Jensen, P.A.; Frandsen, F.J.; Glarborg, P. Release to the Gas Phase of Inorganic Elements during Wood Combustion. Part 1: Development and Evaluation of Quantification Methods. *Energy Fuels* **2006**, *20*, 964–978. [[CrossRef](#)]
22. Boman, C.; Nordin, A.; Boström, D.; Öhman, M. Characterization of Inorganic Particulate Matter from Residential Combustion of Pelletized Biomass Fuels. *Energy Fuels* **2004**, *18*, 338–348. [[CrossRef](#)]
23. Knudsen, J.N.; Jensen, P.A.; Dam-Johansen, K. Transformation and Release to the Gas Phase of Cl, K, and S during Combustion of Annual Biomass. *Energy Fuels* **2004**, *18*, 1385–1399. [[CrossRef](#)]
24. Wang, G.; Jensen, P.A.; Wu, H.; Frandsen, F.J.; Sander, B.; Glarborg, P. Potassium Capture by Kaolin, Part 1: KOH. *Energy Fuels* **2018**, *32*, 1851–1862. [[CrossRef](#)]
25. Wang, G.; Jensen, P.A.; Wu, H.; Frandsen, F.J.; Sander, B.; Glarborg, P. Potassium Capture by Kaolin, Part 2: K<sub>2</sub>CO<sub>3</sub> KCl, and K<sub>2</sub>SO<sub>4</sub>. *Energy Fuels* **2018**, *32*, 3566–3578. [[CrossRef](#)]
26. Johansson, L.S.; Tullin, C.; Leckner, B.; Sjövall, P. Particle emissions from biomass combustion in small combustors. *Biomass Bioenergy* **2003**, *25*, 435–446. [[CrossRef](#)]
27. Steenari, B.-M.; Lundberg, A.; Pettersson, H.; Wilewska-Bien, M.; Andersson, D. Investigation of Ash Sintering during Combustion of Agricultural Residues and the Effect of Additives. *Energy Fuels* **2009**, *23*, 5655–5662. [[CrossRef](#)]
28. Punjak, W.A.; Uberoi, M.; Shadman, F. High-temperature adsorption of alkali vapors on solid sorbents. *Am. Inst. Chem. Eng. J.* **1989**, *35*, 1186–1194. [[CrossRef](#)]
29. Marinkovic, J.; Seemann, M.; Schwebel, G.L.; Thunman, H. Impact of Biomass Ash–Bauxite Bed Interactions on an Indirect Biomass Gasifier. *Energy Fuels* **2016**, *30*, 4044–4052. [[CrossRef](#)]
30. Öhman, M.; Boström, D.; Nordin, A.; Hedman, H. Effect of Kaolin and Limestone Addition on Slag Formation during Combustion of Wood Fuels. *Energy Fuels* **2004**, *18*, 1370–1376. [[CrossRef](#)]
31. *Effect of Fuel Additive Sorbents (Kaolin and Calcite) on Aerosol Particle Emission and Characteristics during Combustion of Pelletized Woody Biomass*; Boman, C.; Boström, D.; Öhman, M. (Eds.) J. Schmid: Florence, Italy, 2008.
32. Steenari, B.-M.; Lindqvist, O. High-temperature reactions of straw ash and the anti-sintering additives Kaolin and Dolomite. *Biomass Bioenergy* **1998**, *14*, 67–76. [[CrossRef](#)]
33. Höfer, I.; Huelsmann, T.; Kaltschmitt, M. Influence of Ca- and Al-additives on the pollutant emissions from blends of wood and straw in small-scale combustion. *Biomass Bioenergy* **2021**, *150*, 106135. [[CrossRef](#)]
34. Lindström, E.; Sandström, M.; Boström, D.; Öhman, M. Slagging Characteristics during Combustion of Cereal Grains Rich in Phosphorus. *Energy Fuels* **2007**, *21*, 710–717. [[CrossRef](#)]
35. Wu, H.; Castro, M.; Jensen, P.A.; Frandsen, F.J.; Glarborg, P.; Dam-Johansen, K.; Røkke, M.; Lundtorp, K. Release and Transformation of Inorganic Elements in Combustion of a High-Phosphorus Fuel. *Energy Fuels* **2011**, *25*, 2874–2886. [[CrossRef](#)]
36. De Fusco, L.; Boucquey, A.; Blondeau, J.; Jeanmart, H.; Contino, F. Fouling propensity of high-phosphorus solid fuels: Predictive criteria and ash deposits characterisation of sunflower hulls with P/Ca-additives in a drop tube furnace. *Fuel* **2016**, *170*, 16–26. [[CrossRef](#)]
37. Novaković, A.; van Lith, S.C.; Frandsen, F.J.; Jensen, P.A.; Holgersen, L.B. Release of Potassium from the Systems K–Ca–Si and K–Ca–P. *Energy Fuels* **2009**, *23*, 3423–3428. [[CrossRef](#)]
38. Höfer, I.; Kaltschmitt, M. Assessment of additives avoiding the release of problematic species into the gas phase during biomass combustion—Development of a fast screening method based on TGA. *Biomass Convers. Biorefinery* **2019**, *9*, 21–33. [[CrossRef](#)]
39. Corcoran, A.; Marinkovic, J.; Lind, F.; Thunman, H.; Knutsson, P.; Seemann, M. Ash Properties of Ilmenite Used as Bed Material for Combustion of Biomass in a Circulating Fluidized Bed Boiler. *Energy Fuels* **2014**, *28*, 7672–7679. [[CrossRef](#)]

40. Dragutinovic, N.; Höfer, I.; Kaltschmitt, M. Effect of additives on thermochemical conversion of solid biofuel blends from wheat straw, corn stover, and corn cob. *Biomass Convers. Biorefinery* **2019**, *9*, 35–54. [CrossRef]
41. Wiinikka, H.; Grönberg, C.; Öhrman, O.; Boström, D. Influence of TiO<sub>2</sub> Additive on Vaporization of Potassium during Straw Combustion. *Energy Fuels* **2009**, *23*, 5367–5374. [CrossRef]
42. Aho, M.; Paakkinen, K.; Taipale, R. Destruction of alkali chlorides using sulphur and ferric sulphate during grate combustion of corn stover and wood chip blends. *Fuel* **2013**, *103*, 562–569. [CrossRef]
43. Kassman, H.; Bäfver, L.; Åmand, L.-E. The importance of SO<sub>2</sub> and SO<sub>3</sub> for sulphation of gaseous KCl—An experimental investigation in a biomass fired CFB boiler. *Combust. Flame* **2010**, *157*, 1649–1657. [CrossRef]
44. Kassman, H.; Pettersson, J.; Steenari, B.-M.; Åmand, L.-E. Two strategies to reduce gaseous KCl and chlorine in deposits during biomass combustion—Injection of ammonium sulphate and co-combustion with peat. *Fuel Process. Technol.* **2013**, *105*, 170–180. [CrossRef]
45. Hu, Z.; Wang, X.; Ruan, R.; Li, S.; Bai, S.; Zhang, J.; Tan, H. Effect of SO<sub>2</sub> Addition on PM Formation from Bio-mass Combustion in an Entrained Flow Reactor. *Energy Fuels* **2018**, *32*, 11030–11037. [CrossRef]
46. Wu, H.; Pedersen, M.N.; Jespersen, J.B.; Aho, M.; Roppo, J.; Frandsen, F.J.; Glarborg, P. Modeling the Use of Sulfate Additives for Potassium Chloride Destruction in Biomass Combustion. *Energy Fuels* **2014**, *28*, 199–207. [CrossRef]
47. Huelsmann, T.; Mack, R.; Kaltschmitt, M.; Hartmann, H. Influence of kaolinite on the PM emissions from small-scale combustion. *Biomass Convers. Biorefinery* **2019**, *9*, 55–70. [CrossRef]
48. Khalil, R.A.; Todorovic, D.; Skreiberg, O.; Becidan, M.; Bac—kman, R.; Goile, F.; Skreiberg, A.; Sørum, L. The effect of kaolin on the combustion of demolition wood under well-controlled conditions. *Waste Manag. Res. J. Int. Solid Wastes Public Clean. Assoc. ISWA* **2012**, *30*, 672–680. [CrossRef]
49. Mack, R.; Kuptz, D.; Schön, C.; Hartmann, H. Combustion behavior and slagging tendencies of kaolin additivated agricultural pellets and of wood-straw pellet blends in a small-scale boiler. *Biomass Bioenergy* **2019**, *125*, 50–62. [CrossRef]
50. Geisen, B.; Givers, F.; Kuptz, D.; Peetz, D.; Schmidt-Baum, T.; Schön, C.; Schreiber, K.; Schulmeyer, F.; Thudium, T.; Zelinski, V.; et al. *Handbuch zum Qualitätsmanagement von Holzhackschnitzeln*; Fachagentur Nachwachsende Rohstoffe e. V. (FNR) and Bundesverband Bioenergie e. V. (BBE): Gülzow-Prüzen, Germany, 2017.
51. Bundesrepublik Deutschland, Bundesministerium für Justiz, Bundesamt für Justiz. *Erste Verordnung zur Durchführung des Bundes-Immissionsschutzgesetzes (Verordnung über kleine und mittlere Feuerungsanlagen—1. BImSchV)*; Bundesministerium für Justiz: Berlin, Germany; Bundesamt für Justiz: Bonn, Germany, 2010.
52. Gollmer, C.; Höfer, I.; Harms, D.; Kaltschmitt, M. Potential additives for small-scale wood chip combustion—Laboratory-scale estimation of the possible inorganic particulate matter reduction potential. *Fuel* **2019**, *254*, 115695. [CrossRef]
53. Gollmer, C.; Weigel, V.; Kaltschmitt, M. Emission Mitigation by Aluminum-Silicate-Based Fuel Additivation of Wood Chips with Kaolin and Kaolinite. *Energies* **2023**, *16*, 3095. [CrossRef]
54. Kaltschmitt, M.; Höfer, I.; Gollmer, C. *Entwicklung, Erprobung und Untersuchung eines innovativen Verfahrens zur Additivierung von Hackschnitzeln zwecks Reduzierung der Emissionen aus Holzfeuerungen*; Deutsche Bundesstiftung Umwelt (DBU): Osnabrück, Germany, 2022.
55. Diedrich, H.; Stahl, A. *NCHS-Elementaranalyse. M02.001. 02*; Technische Universität Hamburg, Zentrallabor Chemische Analytik: Hamburg, Germany, 2021.
56. Fütterer, C.; Stahl, A. *Elementbestimmung mit ICP-OES. M02.015. 03*; Technische Universität Hamburg, Zentrallabor Chemische Analytik: Hamburg, Germany, 2021.
57. Cöllen, H.; Frerichs, H.; Stahl, A. *Elementbestimmung per ICP-MS. M02.013. 01*; Technische Universität Hamburg, Zentrallabor Chemische Analytik: Hamburg, Germany, 2021.
58. *Deutsches Institut für Normung e. V. DIN EN ISO 17225-1*; Biogene Festbrennstoffe—Brennstoffspezifikationen und -klassen—Teil 1: Allgemeine Anforderungen. Beuth Verlag GmbH: Berlin, Germany, 2014.
59. *Deutsches Institut für Normung e. V. DIN EN ISO 17225-4*; Biogene Festbrennstoffe—Brennstoffspezifikationen und -klassen—Teil 4: Klassifizierung von Holzhackschnitzeln. Beuth Verlag GmbH: Berlin, Germany, 2014.
60. Nordin, A. Chemical elemental characteristics of biomass fuels. *Biomass Bioenergy* **1994**, *6*, 339–347. [CrossRef]
61. Bale, C.W.; Bélisle, E.; Chartrand, P.; Decterov, S.A.; Eriksson, G.; Gheribi, A.E.; Hack, K.; Jung, I.-H.; Kang, Y.-B.; Melançon, J.; et al. FactSage thermo-chemical software and databases, 2010–2016. *Calphad* **2016**, *54*, 35–53. [CrossRef]
62. Gebrüder Dorfner GmbH & Co. *Kaolin- und Kristallquarzsand-Werke KG: Sicherheitsdatenblatt—Kaolin Gemahlen*; Gebrüder Dorfner GmbH & Co.: Hirschau, Germany, 2018.
63. Andrea Wolbring GmbH & Co. KG: Anorthit, Anzing. Available online: <https://shop.keramikbedarf-online.de/Anorthit/24001> (accessed on 28 August 2024).
64. Andrea Wolbring GmbH & Co. KG: Tonerdehydrat, Anzing. Available online: <https://shop.keramikbedarf-online.de/Tonerdehydrat/2440> (accessed on 28 August 2024).
65. Merck KGaA. *Sicherheitsdatenblatt—Titan(IV)-oxid*; Merck KGaA: Darmstadt, Germany, 2022.
66. Heizomat—Gerätebau + Energiesysteme GmbH. *Technische Daten RHK-AK 30*; Heizomat—Gerätebau + Energiesysteme GmbH: Gunzenhausen, Germany, 2021.

67. Deutsches Institut für Normung e. V. DIN EN 15259; Luftbeschaffenheit—Messung von Emissionen aus Stationären Quellen—Anforderungen an Messstrecken und Messplätze und an die Messaufgabe, den Messplan und den Messbericht. Beuth Verlag GmbH: Berlin, Germany, 2008.
68. Deutsches Institut für Normung e. V. DIN EN 13284-1; Emissionen aus Stationären Quellen—Ermittlung der Staubmassenkonzentration bei Geringen Staubkonzentrationen—Teil 1: Manuelles Gravimetrisches Verfahren. Beuth Verlag GmbH: Berlin, Germany, 2018.
69. Verein Deutscher Ingenieure e. V. VDI 2066 Blatt 1; Messen von Partikeln—Staubmessung in Strömenden Gasen—Gravimetrische Bestimmung der Staubbiladung. Beuth Verlag GmbH: Berlin, Germany, 2019.
70. Deutsches Institut für Normung e. V. DIN 22022-1; Feste Brennstoffe—Bestimmung der Gehalte an Spurenelementen—Teil 1: Allgemeine Regeln, Probenahme und Probenvorbereitung—Vorbereitung der Analysenprobe für die Bestimmung (Aufschlussverfahren). Beuth Verlag GmbH: Berlin, Germany, 2014.
71. Deutsches Institut für Normung e. V. DIN 22022-3; Feste Brennstoffe—Bestimmung der Gehalte an Spurenelementen—Teil 3: AAS-Flammentechnik. Beuth Verlag GmbH: Berlin, Germany, 2001.
72. Deutsches Institut für Normung e. V. DIN 38406 Teil 13; Deutsche Einheitsverfahren zur Wasser-, Abwasser- und Schlammuntersuchung—Kationen (Gruppe E)—Bestimmung von Kalium mittels Atomabsorptionsspektrometrie (AAS) in der Luft-Acetylen-Flamme (E 13). Beuth Verlag GmbH: Berlin, Germany, 1992.
73. Deutsches Institut für Normung e. V. DIN 38406 Teil 14; Deutsche Einheitsverfahren zur Wasser-, Abwasser- und Schlammuntersuchung—Kationen (Gruppe E)—Bestimmung von Natrium Mittels Atomabsorptionsspektrometrie (AAS) in der Luft-Acetylen-Flamme (E14). Beuth Verlag GmbH: Berlin, Germany, 1992.
74. Deutsches Institut für Normung e. V. DIN EN ISO 7980; Wasserbeschaffenheit—Bestimmung von Calcium und Magnesium—Verfahren mittels Absorptionsspektrometrie. Beuth Verlag GmbH: Berlin, Germany, 2000.
75. Deutsches Institut für Normung e. V. DIN EN ISO 10304-1; Wasserbeschaffenheit—Bestimmung von Gelösten Anionen Mittels Flüssigkeits-Ionenchromatographie—Teil 1: Bestimmung von Bromid, Chlorid, Fluorid, Nitrat, Nitrit, Phosphat und Sulfat. Beuth Verlag GmbH: Berlin, Germany, 2009.
76. Tritscher, T.; Koched, A.; Han, H.-S.; Filimundi, E.; Johnson, T.; Elzey, S.; Avenido, A.; Kykal, C.; Bischof, O.F. Multi-Instrument Manager Tool for Data Acquisition and Merging of Optical and Electrical Mobility Size Distributions. *J. Phys. Conf. Ser.* **2014**, *617*, 012013. [[CrossRef](#)]
77. Deutsches Institut für Normung e. V. DIN EN ISO 16967; Biogene Festbrennstoffe—Bestimmung von Hauptelementen—Al, Ca, Fe, Mg, P, K, Si, Na und Ti. Beuth Verlag GmbH: Berlin, Germany, 2015.
78. Deutsches Institut für Normung e. V. DIN EN ISO 16968; Biogene Festbrennstoffe—Bestimmung von Spurenelementen. Beuth Verlag GmbH: Berlin, Germany, 2015.
79. Deutsches Institut für Normung e. V. DIN EN 13925-1; Zerstörungsfreie Prüfung—Röntgendiffraktometrie von Polykristallinen und Amorphen Materialien—Teil 1: Allgemeine Grundlagen. Beuth Verlag GmbH: Berlin, Germany, 2003.
80. Deutsches Institut für Normung e. V. DIN EN 13925-2; Zerstörungsfreie Prüfung—Röntgendiffraktometrie von Polykristallinen und Amorphen Materialien—Teil 2: Verfahrensabläufe. Beuth Verlag GmbH: Berlin, Germany, 2003.
81. Gollmer, C.; Höfer, I.; Kaltschmitt, M. Laboratory-scale additive content assessment for aluminum-silicate-based wood chip additivation. *Renew. Energy* **2021**, *164*, 1471–1484. [[CrossRef](#)]
82. Obernberger, I.; Brunner, T.; Baernthaler, G. Fine particulate emissions from modern Austrian small-scale biomass combustion plants. In Proceedings of the 15th European Biomass Conference and Exhibition for Research to Market Deployment: For Research to Market Deployment, Berlin, Germany, 11 May 2007.
83. Ebert, F. Particle separation for biomass combustion. In *Aerosols from Biomass Combustion*; Nussbaumer, T., Ed.; Verenum: Zürich, Switzerland, 2001.
84. Obernberger, I.; Brunner, T.; Jöller, M. Characterisation and formation of aerosols and fly-ashes from fixed-bed biomass combustion. In *Aerosols from Biomass Combustion*; Nussbaumer, T., Ed.; Verenum: Zürich, Switzerland, 2001.
85. Hueglin, C.; Gaegauf, C.; Künzel, S.; Burtscher, H. Characterization of Wood Combustion Particles: Morphology, Mobility, and Photoelectric Activity. *Environ. Sci. Technol.* **1997**, *31*, 3439–3447. [[CrossRef](#)]
86. Leskinen, J.; Tissari, J.; Uski, O.; Virén, A.; Torvela, T.; Kaivosoja, T.; Lamberg, H.; Nuutinen, I.; Kettunen, T.; Joutsensaari, J.; et al. Fine particle emissions in three different combustion conditions of a wood chip-fired appliance—Particulate physicochemical properties and induced cell death. *Atmos. Environ.* **2014**, *86*, 129–139. [[CrossRef](#)]
87. Nussbaumer, T. *Aerosols from Biomasse Combustion—Technical Report on Behalf of the IEA Bioenergy Task 32*; IEA Bioenergy: Zurich, Germany, 2017.
88. Tissari, J.; Lyyränen, J.; Hytönen, K.; Sippula, O.; Tapper, U.; Frey, A.; Saarnio, K.; Pennanen, A.S.; Hillamo, R.; Salonen, R.O.; et al. Fine particle and gaseous emissions from normal and smouldering wood combustion in a conventional masonry heater. *Atmos. Environ.* **2008**, *42*, 7862–7873. [[CrossRef](#)]
89. Bäfver, L.S.; Rönnbäck, M.; Leckner, B.; Claesson, F.; Tullin, C. Particle emission from combustion of oat grain and its potential reduction by addition of limestone or kaolin. *Fuel Process. Technol.* **2009**, *90*, 353–359. [[CrossRef](#)]
90. Schmidt, G.; Trouvé, G.; Leyssens, G.; Schönnenbeck, C.; Genevray, P.; Cazier, F.; Dewaele, D.; Vandenbilcke, C.; Faivre, E.; Denance, Y.; et al. Wood washing: Influence on gaseous and particulate emissions during wood combustion in a domestic pellet stove. *Fuel Process. Technol.* **2018**, *174*, 104–117. [[CrossRef](#)]

91. Chanpirak, A.; Hashemi, H.; Frandsen, F.J.; Wu, H.; Glarborg, P.; Marshall, P. The chemical coupling between moist CO oxidation and gas-phase potassium sulfation. *Fuel* **2023**, *336*, 127127. [[CrossRef](#)]
92. Glarborg, P. Hidden interactions—Trace species governing combustion and emissions. *Proc. Combust. Inst.* **2007**, *31*, 77–98. [[CrossRef](#)]
93. Hindiyarti, L.; Frandsen, F.; Livbjerg, H.; Glarborg, P. Influence of potassium chloride on moist CO oxidation under reducing conditions: Experimental and kinetic modeling study. *Fuel* **2006**, *85*, 978–988. [[CrossRef](#)]
94. Chanpirak, A.; Wu, H.; Glarborg, P.; Marshall, P. An experimental and chemical kinetic modeling study of the role of potassium in the moist oxidation of CO. *Fuel* **2023**, *335*, 127075. [[CrossRef](#)]
95. Siegmund, T.; Gollmer, C.; Scherzinger, M.; Kaltschmitt, M. A review of CO emissions during solid biofuel combustion—Formation mechanisms and fuel-related reduction measures. *J. Energy Inst.* **2024**, *116*, 101762. [[CrossRef](#)]
96. Siegmund, T.; Gollmer, C.; Horstmann, N.; Kaltschmitt, M. Carbon monoxide (CO) and particulate matter (PM) emissions during the combustion of wood pellets in a small-scale combustion unit—Influence of aluminum-(silicate-)based fuel additivation. *Fuel Process. Technol.* **2024**, *262*, 108111. [[CrossRef](#)]
97. Vassilev, S.V.; Baxter, D.; Vassileva, C.G. An overview of the behaviour of biomass during combustion: Part I. Phase-mineral transformations of organic and inorganic matter. *Fuel* **2013**, *112*, 391–449. [[CrossRef](#)]

**Disclaimer/Publisher’s Note:** The statements, opinions and data contained in all publications are solely those of the individual author(s) and contributor(s) and not of MDPI and/or the editor(s). MDPI and/or the editor(s) disclaim responsibility for any injury to people or property resulting from any ideas, methods, instructions or products referred to in the content.